Systematic Approaches to Determining Degradation Rates from Continuous Meteorological and System Production Data

2012 PV Module Reliability Workshop, NREL, Golden, Colorado, February 28-29, 2012

Kenneth J. Sauer

1.

BACKGROUND

- Project size and financing are governed by the confidence investors have in the projected energy production of a photovoltaic (PV) system over the term of its power purchase agreement or planned asset lifetime.
- Production estimates are largely a function of anticipated annual degradation rates (R_d), which are known to vary within and across PV technologies and systems.
- The ability to more accurately and objectively quantify degradation rates is fundamental toward yielding more favorable energy production exceedance probabilities and improving the overall financial viability of large-scale PV.

APPROACH

- Systematic approaches in qualifying and translating raw, continuous meteorological and system production data into performance time series are developed for the purpose of identifying linear trends in PV system performance as a function of time (R_d).
- The developed approaches are implemented using data from a large-scale, commercial PV array of multicrystalline silicon modules in operation for over 2.5 years.
- Initial steps toward model validation are taken through measurements conducted on a sample of modules after two years of outdoor exposure.

REFERENCES

1. D. L. King, W. E. Boyson, J.A. Kratochvil, "Photovoltaic array performance model", Sandia National Laboratories Publication #SAND2004-3535, August 2004.
2. STC: 1,000W/m² global POA irradiance (G_{STC}), 25°C module temperature (T_{STC}), AM1.5 spectrum according to EN 60904-3.
3. International Standard IEC 61724. Photovoltaic system performance monitoring – Guidelines for measurement, data exchange and analysis, First Ed., International Electrotechnical Commission (IEC), Geneva, April 1998.
4. List of Eligible Inverters per SB1 Guidelines – Go Solar California. (2011). Retrieved, May 23, 2011, from http://www.gosolarcalifornia.org/equipment/inverters.php.

2.

Meteorological & Production Data

- For implementing (and reporting on) approaches in R_d analysis, 2.5 years of non-spectrally corrected data with a 1-min sampling interval (τ_s) are used. Data at each τ_s include date, time, system AC energy output (E_{AC}, kWh), instantaneous global plane-of-array irradiance (G_{POA}, W/m²), instantaneous module temperature (T_{MOD}, °C) and instantaneous ambient temperature (T_{AMB}, °C).
- Nominal uncertainties of G_{POA}, T_{MOD} and T_{AMB} measurements are ±5%, ±0.5°C, and ±0.3°C, respectively. A calibrated silicon photodiode pyranometer and temperature sensor fixed to the backsheet behind a cell were used to measure G_{POA} and T_{MOD}, respectively.
- A kWh meter was used to measure E_{AC} at the combined output of (5) inverters.

Cell Temperature Model

- Eq. 1 is used to convert T_{MOD} to cell temperature (T_{CELL}, °C) at each indexed τ_s. The difference between backsheet and cell temperature (ΔT) is 3°C for the modules in the chosen system [1, 2].

$$(1)\quad T_{CELL,i,\tau_s} = T_{MOD,i,\tau_s} + \left(\frac{G_{POA,i,\tau_s}}{G_{STC}}\right)\cdot\Delta T$$

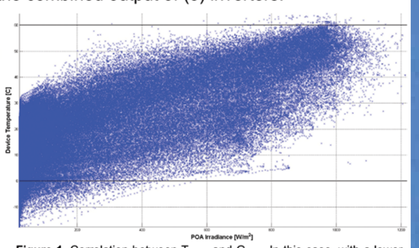

Figure 1. Correlation between T_{CELL} and G_{POA}. In this case, with a lower data acceptance criterion of G_{POA} in place (for example, G_{POA}≥700W/m²), T_{CELL} is effectively constrained to 0-60°C.

Energy Models

- G_{POA} and E_{AC} are used to derive insolation (H_{POA}, Wh/m²) and power (P_{AC}, kW), respectively, over each τ_s per IEC 61724-1 Section 8 [3].

3.

Inverter Efficiency Model

- The nominal module MPP voltage and temperature coefficient of voltage (β_{Vmpp}=-0.46%/°C) are used to derive operating system voltage from T_{CELL} and the series string size, N_s (Eq. 2) [2].

$$V_{mpp,SYST,i,\tau_s} = N_S \times V_{mpp,Nom,MOD} \times \left[1 + \beta_{Vmpp}\cdot\left(T_{CELL,i,\tau_s} - T_{STC}\right)\right] \quad (2)$$

- An empirical, 2-D cubic-spline interpolation-based model (f_I) describing inverter efficiency as a function of power and input voltage is used to translate AC to DC production data (Eq. 3, Fig. 2). Inverter performance data made public by the California Energy Commission and California Public Utilities Commission (CEC & CPUC) provides the basis for the model [4]. DC energy (E_{DC}, kW) is derived from P_{DC} per IEC 61724-1 Section 8 [3].

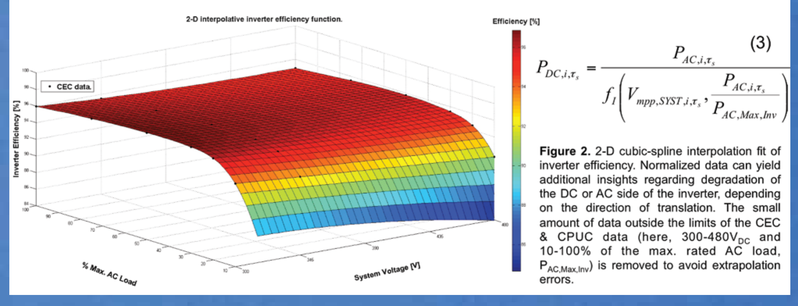

$$P_{DC,i,\tau_s} = \frac{P_{AC,i,\tau_s}}{f_I\left(V_{mpp,SYST,i,\tau_s}, \frac{P_{AC,i,\tau_s}}{P_{AC,Max,Inv}}\right)} \quad (3)$$

Figure 2. 2-D cubic-spline interpolation fit of inverter efficiency. Normalized data can yield additional insights regarding degradation of the DC or AC side of the inverter, depending on the direction of translation. The small amount of data outside the limits of the CEC & CPUC data (here, 300-480V_{DC} and 10-100% of the max. rated AC load, $P_{AC,Max,Inv}$) is removed to avoid extrapolation errors.

4.

Recording Interval

- A data recording interval (τ_r, where $\tau_r \geq \tau_s$) is user-defined (here, 5-min is used). E and H_{POA} at each τ_s are summed over each indexed τ_r, while P, T_{AMB}, T_{CELL}, and G_{POA} are averaged.

Performance Model

- System efficiency (η_{DC}, Eq. 4) is calculated over each τ_r [2].

$$\eta_{DC,i,\tau_r} = \frac{E_{DC,i,\tau_r}}{H_{POA,i,\tau_r}\cdot A_{SYST}} \quad (4)$$

Power Temperature Coefficient

- The temperature coefficient of MPP power (γ_{Pmpp}) is derived from the slope of η_{DC} vs. T_{CELL} following a robust linear regression fit (Fig. 3). In Fig. 4, γ_{Pmpp} is shown to vary when the lower data acceptance limit of G_{POA} is set at a level <700W/m².

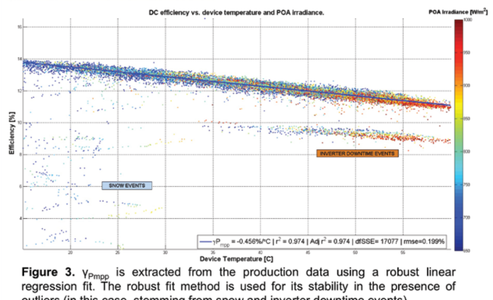

Figure 3. γ_{Pmpp} is extracted from the production data using a robust linear regression fit. The robust fit method is used for its stability in the presence of outliers (in this case, stemming from snow and inverter downtime events).

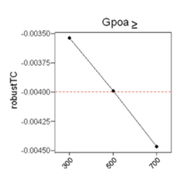

γ_{Pmpp} (G_{POA}≥800W/m²) = -0.458%/°C
γ_{Pmpp} (G_{POA}≥900W/m²) = -0.462%/°C

Figure 4. The response of γ_{Pmpp} to the lower G_{POA} filtration cutoff (with the upper limit fixed at 1,000W/m²) is demonstrated with a main effects plot. γ_{Pmpp} remains highly stable for lower data acceptance limits ≥700W/m². In this work, a lower limit of 700W/m² is applied.

5.

STC Rating

$$(5)\quad E_{DC,STC-Adj,i,\tau_r} = \frac{E_{DC,i,\tau_r}}{\left(\frac{H_{POA,i,\tau_r}}{H_{STC}}\right)\cdot\left[1+\gamma_{Pmpp}\cdot\left(T_{CELL,i,\tau_r} - T_{STC}\right)\right]}$$

$$(6)\quad E_{DC,STC} = f_H(H_{STC})$$

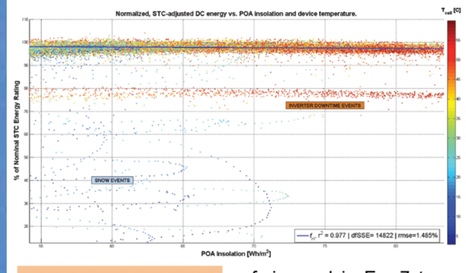

Figure 5. $E_{DC,STC-Adj}$ (normalized to the nominal rating) is plotted vs. H_{POA} (and T_{CELL}). A robust linear regression is used to fit $E_{DC,STC-Adj}$ over the range of device linearity (700W/m²≤G_{POA}≤1,000W/m²). Substitution of H_{STC} into f_H (Eq. 6) yields an approximation of the system energy rating at STC that can be applied in Eq. 7.

- A robust linear fit of STC-adjusted E_{DC} ($E_{DC,STC-Adj}$, kW, Eq. 5) vs. H_{POA} over the range of device linearity (Fig. 5) is used to approximate performance at STC (Eq. 6) for use in Eq. 7 [2]. H_{STC} is derived from G_{STC} over τ_r following IEC 61724-1 Section 8 [2, 3].

Relative Efficiency Delta from STC

- f_H is used in Eq. 7 to compute the relative efficiency deviation (delta) from STC ($\Delta\eta_{DC,STC}$) over each indexed τ_r [2]. R_d can be extracted from a linear fit of $\Delta\eta_{DC,STC}$ vs. time (Fig. 6, Eq. 10).

$$\Delta\eta_{DC,STC,i,\tau_r} = \left\{\frac{E_{DC,i,\tau_r}}{f_H(H_{STC})\cdot\left(\frac{H_{POA,i,\tau_r}}{H_{STC}}\right)\cdot\left[1+\gamma_{Pmpp}\cdot\left(T_{CELL,i,\tau_r} - T_{STC}\right)\right]}\right\} - 1 \quad (7)$$

6.

Irradiance Transience Model

- An irradiance transience allowance criterion (ΔG_{POA}) is applied within each τ_r (Eqs. 8-9, Fig. 6) to remove unrepresentative data from imprecise measurements collected during transient (cloudy) ambient conditions. A robust linear regression is used to extract R_d using Eq. 10, where N_τ is a time index multiplier.

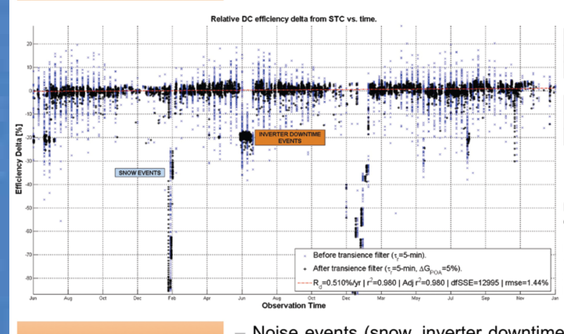

$$\left[\frac{\max(G_{POA,i,\tau_r} \geq 0)}{\min(G_{POA,i,\tau_r} > 0)}\right] \leq 1 + \Delta G_{POA} \quad (8)$$

$$\left[\frac{\min(G_{POA,i,\tau_r} \geq 0)}{\max(G_{POA,i,\tau_r} > 0)}\right] \geq 1 - \Delta G_{POA} \quad (9)$$

$$R_d\left(\frac{\%}{yr}\right) = \left(\frac{N_\tau \cdot m}{b}\right)\cdot 100 \quad (10)$$

N_τ=1 (yr.), 12 (mo.), 52 (week), 365 (day), depending on the reporting interval (τ).

Figure 6. $\Delta\eta_{DC,STC}$ vs. time, with 1.) no transience filter applied, and 2.) ΔG_{POA}=5%. R_d is reported for case (2).

Noise Events

- Noise events (snow, inverter downtime) are removed prior to final analysis of R_d. Filtration criteria based around the median $\Delta\eta_{DC,STC}$ can in some cases be applied as a categorical filter.

Reporting Intervals

- Final system R_d results are derived from η_{DC} time series (Eq. 4), computed over daily, weekly and monthly reporting intervals (τ).

7.

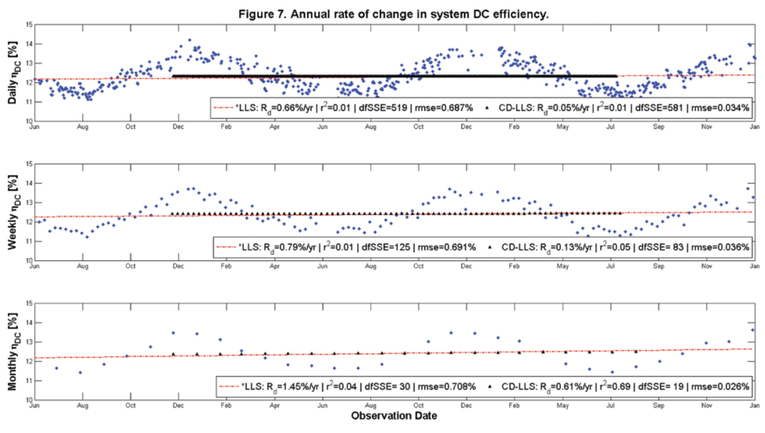

- The time series of η_{DC} at each indexed τ are plotted. Simple linear least squares fit (LLS) is used to derive R_d (Eq. 10). *With LLS, it is best if data begins and ends at the same time of year, to avoid seasonality effects – note that Fig. 7 includes the full data set (2.5 years).
- Classical decomposition (CD) method is applied to deseasonalize the η_{DC} time series, ideally such that all available data can be used. Centered moving averages are computed over periods of N_τ. Moving average time series are fit using LLS to derive R_d (CD-LLS).

8.

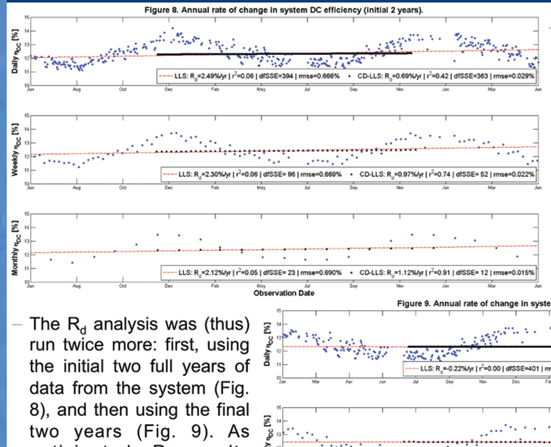

- In this case, resultant positive R_d values (Figs. 6-7) were thought to relate to a faulty inverter that was repaired on two occasions during the initial "wear-in" period of system operation. Since DC production data was derived (Eq. 3), such effects would still be present in the data.
- The R_d analysis was (thus) run twice more: first, using the initial two full years of data from the system (Fig. 8), and then using the final two years (Fig. 9). As anticipated, R_d results converged toward a more positive rate in the first two years, and a more negative rate in the final two years.

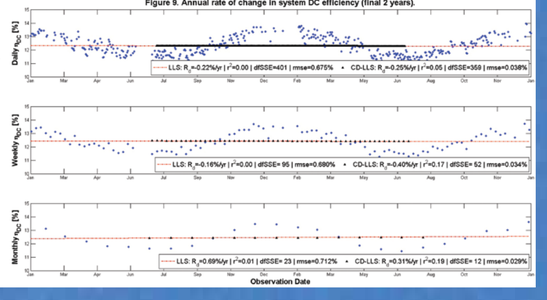

9.

Model Validation

- A first model validation effort was carried out through testing a sample of modules (n=32) from the same system after two years in operation (t), according to the on-site (field) and laboratory protocols outlined in Fig. 10. Module R_d results are computed using Eq. 11 and summarized statistically in Fig. 11.

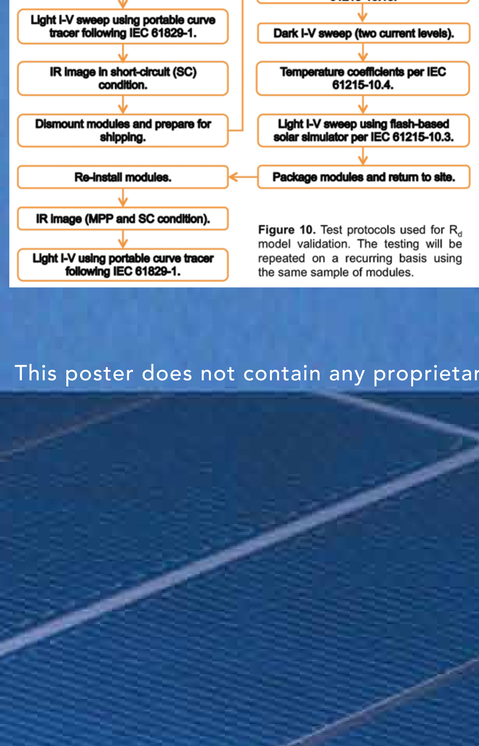

Figure 10. Test protocols used for R_d model validation. The testing will be repeated on a recurring basis using the same sample of modules.

$$R_d\left(\frac{\%}{yr}\right) = \left[\frac{\left(\frac{P_t - P_0}{t}\right)\cdot N_\tau}{P_0}\right]\cdot 100 \quad (11)$$

Avg.=-0.26%/yr, Med.=-0.35%/yr

Figure 11. Boxplot of module R_d values calculated using Eq. 11, where the initial power, P_0, represents light-stabilized, factory-tested values, and the power after two years of operation, P_t, is based on indoor laboratory measurements. Results align well with R_d derived from the model using the final two years of data from the chosen system.

Yingli Americas